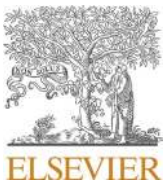
Ecological Informatics 96 (2026) 103863



Contents lists available at ScienceDirect

Ecological Informatics

journal homepage: www.elsevier.com/locate/ecolinf





# Variation in foliar chlorophyll *a*nd carotenoid contents of European aspen: Effect of forest structure and estimation by airborne hyperspectral imaging

Sarita Keski-Saari [a,b,*], Markku Keinänen [b,c], Janne Mäyrä [d], Arto Viinikka [e,1], Topi Tanhuanpää [a,f,2], Sonja Kivinen [a], Laura Poikolainen [a,3], Ehsan Khoramshahi [a], Petteri Vihervaara [g], Timo Kumpula [a]

[a] Department of Geographical and Historical Studies, University of Eastern Finland, P.O. Box 111, FI-80101 Joensuu, Finland
[b] University of Eastern Finland, Department of Environmental and Biological Sciences, P.O. Box 111, FI-80101 Joensuu, Finland
[c] University of Eastern Finland, Center for Photonics Sciences, P.O. Box 111, FI-80101 Joensuu, Finland
[d] Finnish Environment Institute (Syke), Quality of Information, Latokartanonkaari 11, FI-00790 Helsinki, Finland
[e] Finnish Environment Institute (Syke), Built Environment Solutions Unit, Latokartanonkaari 11, FI-00790 Helsinki, Finland
[f] University of Helsinki, Department of Forest Sciences, Helsinki FI-00014, Finland
[g] Finnish Environment Institute (Syke), Nature Solutions, Latokartanonkaari 11, FI-00790 Helsinki, Finland

ARTICLE INFO

*Keywords:*
*Populus tremula*
Intraspecific diversity
Chlorophyll
Carotenoids
Airborne hyperspectral imaging

ABSTRACT

Foliar chlorophyll (Chl) and carotenoid (Car) contents are essential physiological traits that reflect plant health. We investigated variation in these pigments in the upper crowns of European aspen (*Populus tremula*), a keynote species that supports high biodiversity in boreal forests through its ecological functions. We examined how Chl and Car contents vary with protection status and forest structural characteristics by airborne laser scanning (ALS) and assessed the potential of airborne hyperspectral imaging (HSI, 432- 810 nm) in combination with ALS to estimate single crown pigment distributions at the landscape level. Leaf-area based Chl and Car contents showed substantial variation. High Chl and Car content in protected zone was unexpected considering the older average age of the aspens. Tree and stand structural characteristics influenced intraspecific diversity of pigment contents. In non-protected and roadside zones, lower pigment content co-occurred with the higher tree density, which implies influence of shading by neighboring trees. Random forest (RF) model using spectral indices allowed estimation of Chl content from hyperspectral reflectance with coefficient of determination ($R^2$) of 0.52 and relative root mean square errors (RMSE%) of 11.7%, whereas accuracy was slightly less for partial least squares regression (PLSR) ($R^2$ 0.51 and RMSE 13.4%). For Car content, the accuracies were lower (for PLSR $R^2$ 0.32 and RMSE% 13.5 and for RF $R^2$ 0.28 and RMSE% 13.23). Overall, the intraspecific diversity of pigment contents of a keynote species was high, and influenced by structural diversity of forests, which can have ecological consequences for the ecosystem level biodiversity in boreal forests.

## 1. Introduction

Biodiversity loss driven by land-use changes and the prevailing climate change is a major global concern (Dasgupta, 2021). Therefore, there is a need to develop operational biodiversity monitoring products such as remote sensing-based biodiversity indicators for large area coverage. Essential remote sensing-based biodiversity variables have been proposed as such metrics (Skidmore et al., 2021). While biodiversity is often equated with species diversity, intraspecific diversity, i.e., variation among individuals of the same species, can play an important role in ecosystems (Whitham et al., 2006). In forest ecosystems, such diversity contributes to structural diversity through traits like

* Corresponding author at: Department of Geographical and Historical Studies, University of Eastern Finland, P.O. Box 111, FI-80101 Joensuu, Finland.
*E-mail addresses:* sarita.keski-saari@uef.fi (S. Keski-Saari), markku.keinanen@uef.fi (M. Keinänen), janne.mayra@syke.fi (J. Mäyrä), arto.viinikka@maanmittauslaitos.fi (A. Viinikka), topi.tanhuanpaa@uef.fi (T. Tanhuanpää), sonja.kivinen@uef.fi (S. Kivinen), laura.poikolainen@ely-keskus.fi (L. Poikolainen), petteri.vihervaara@syke.fi (P. Vihervaara), timo.kumpula@uef.fi (T. Kumpula).
[1] Present address: National Land Survey of Finland, Basic Spatial Data Services, P.O. Box 84, FI-00521 Helsinki, Finland.
[2] Present address: Finnish Environment Institute (Syke), Nature Solutions, Latokartanonkaari 11, FI-00790 Helsinki, Finland.
[3] Present address: Finnish Supervisory Agency, Environment, P.O. Box 69, FI-80101 Joensuu, Finland.

https://doi.org/10.1016/j.ecoinf.2026.103863
Received 21 October 2025; Received in revised form 24 April 2026; Accepted 25 May 2026
Available online 26 May 2026
1574-9541/© 2026 The Authors. Published by Elsevier B.V. This is an open access article under the CC BY license (http://creativecommons.org/licenses/by/4.0/).

tree height and crown size (LaRue et al., 2023), and to functional diversity, such as genotypic variation in leaf pigment content (Deepak et al., 2020). Genotypic differences in leaf physiological and chemical traits can further influence ecosystem processes, including litter decomposition and community structure (Madritch et al., 2014), and enhance population resilience to environmental disturbances (Whitham et al., 2006).

Chlorophyll a and b are the main light-absorbing pigments in plant leaves that enable photosynthesis. Foliar chlorophyll (hereafter Chl) content is a useful indicator of plant health and vigor (Croft et al., 2017), and low Chl content is typical under stress conditions (Nestola et al., 2018). Chl content has been suggested as essential biodiversity variable due to its role in ecosystem function and as species-specific trait. Chl content is associated with photosynthetic rate (Chou et al., 2020), photosynthetic capacity (Croft et al., 2017), and gross primary productivity (Li et al., 2018a). Chl content exhibits a positive curvilinear relationship with photosynthetically active radiation absorbed by plant tissues, indicating that it predominantly determines the proportion of incoming light a leaf can absorb (Evans and Poorter, 2001; Niinemets, 2010). Carotenoids accompany chlorophyll in light-harvesting pigment-protein complexes and contribute to light absorption in photosynthesis and prevention of damage by excess light through non-photochemical quenching (Hashimoto et al., 2016). Chlorophyll a and b absorb light mainly in the blue and blue-green (420–520 nm) range and the red (630–680 nm) range, whereas carotenoids absorb primarily in the 410–540 nm range. These patterns of absorption contribute to reflectance features that are characteristic of plants: low reflectance in the blue and red range, a peak in the green range, a sharp increase at the red edge (ca. 700 nm), and high reflectance in the near-infrared (NIR) range (Gates et al., 1965).

Pigment content can be indirectly estimated from leaf and canopy spectral reflectance to enable large-scale monitoring (Croft et al., 2014; Croft and Chen, 2018; Zarco-Tejada et al., 2005), in which traditional chemical methods are too labor-intensive and slow. Pigment estimation from spectral reflectance advanced first through proximal sensing, using band-based indices, such as simple ratio $SR_{705}$ ($R_{750}$ / $R_{705}$, where $R$ denotes reflectance) (Blackburn, 1998; Sims and Gamon, 2002). These indices typically combine bands sensitive and insensitive to pigments, often as ratios or normalized differences (Blackburn, 1998; Sims and Gamon, 2002). For carotenoid (Car) content estimation, indices have been less accurate, which is largely due to overlap in absorbance range with Chl, as well as higher content of Chl in comparison to Car (Blackburn, 1998). Spectral reflectance has successfully been utilized in Chl content estimation in forest environments as full spectrum by Partial least squares regression (PLSR) models (Chen et al., 2022; Serbin et al., 2014).

Hyperspectral imaging (HSI) records reflected light intensity across continuous narrow spectral bands for each image pixel. Most studies on Chl content estimation by airborne HSI have been implemented on forest canopy level, often comprising several tree species (Asner et al., 2015; Asner and Martin, 2008). Individual tree crowns have been addressed rarely, and mostly for conifers (Lin et al., 2019). Airborne laser scanning (ALS) enables mapping of forest structure and individual tree crowns in three dimensions. Combining this tree crown structure information to HSI based spectral knowledge provides the possibility of more accurate tree species identification (Alonzo et al., 2014; Mäyrä et al., 2021) to produce tree maps showing, e.g., the location, size, and species for each tree (e.g., Mäyrä et al., 2021). The tree maps can be further used in characterizing the surroundings of individual trees, showing e.g., the density or mean height of surrounding tree crowns (Palmroos et al., 2023). ALS and HSI have been used in combination to investigate functional diversity (Kamoske et al., 2021) and tree species diversity (Mäyrä et al., 2021; Zhao et al., 2018), but, however, rarely (see Lin et al., 2019) to investigate intraspecific diversity of pigment contents at individual tree level on wide spatial scales.

Diversity of pigment contents influences the quality of the foliage as a resource for the consumer communities, such as herbivores, and can thus influence biodiversity widely at the ecosystem level. For example, higher intraspecific genetic diversity in a plant stand coincides with higher species richness of the arthropod community (Koricheva and Hayes, 2018). Chl and Car contents commonly covary but their contents and ratio may be influenced by environmental conditions (Chen et al., 2022; He et al., 2023). These are, in turn, influenced by forest and tree structural characteristics, but the impacts of forest structure on pigment content remain poorly understood. *Nothofagus nitida* saplings in evergreen temperate rain forest have been reported to have higher Chl content in taller saplings (Coopman et al., 2011), but more detailed knowledge of forest structure effects on pigment content in trees is largely lacking.

European aspen (*Populus tremula* L., hereafter aspen) is a keystone species and an important indicator for biodiversity in boreal forests (Kivinen et al., 2020; Rogers et al., 2020). It provides habitat and food resources for over 750 associated or dependent species, including many rare and red-listed insects, epiphytic lichens, and polypore fungi (Kouki et al., 2004; Tikkanen et al., 2006). Aspen is a light-demanding, early successional tree that regenerates efficiently through root sprouts. It has a scattered distribution within forest landscapes (Kouki et al., 2004; Latva-Karjanmaa et al., 2007), yet it is widely distributed across Eurasia (Kusbach et al., 2024), making it ecologically important over a broad geographic range. In Nordic countries, forest management practices typically favor coniferous trees, which has led to reduced species and structural diversity in forests and a decline in shade-intolerant deciduous trees, particularly aspen (Hardenbol et al., 2020; Kouki et al., 2004).

In this study, we focused on intraspecific diversity of Chl and Car contents in a single keystone tree species, European aspen, at individual tree level, using the combination of HSI and ALS data. The study area in boreal forest region in Finland covered a mosaic of forests with different management intensities, comprising protected, non-protected, and roadside zones. This allowed a wide variation in structural parameters in the forests. We analyzed the Chl and Car contents in the upper crown leaves by traditional laboratory methods and compared them with the crown spectral reflectance acquired by HSI. We also examined relations of aspen crown foliage Chl and Car content to forest and tree structural parameters. We aimed to answer the following questions:

1) How does intraspecific diversity of foliar chlorophyll (Chl) and carotenoid (Car) contents in European aspen vary across forests with differing management intensities?
2) How do tree-level (e.g., diameter at breast height (DBH), height, crown length) and stand-level (e.g., tree density, mean height, top dominance) structural characteristics influence foliar Chl and Car contents in European aspen?
3) How well does airborne HSI combined with ALS allow for estimation of foliar Chl and Car contents of a single, keystone tree species on a wide spatial scale?

## 2. Materials and methods

### 2.1. Study region

The study region encompassed protected and non-protected areas, comprising pristine old forests and managed forests, respectively, within an 83 $km^2$ area in Evo, Hämeenlinna district, southern Finland (Fig. 1). Roadside was defined as with <25 m to the road. Roadside trees were grouped separately because roads affect the light conditions of the trees. Roadsides were considered as a single group regardless of whether inside a protected or non-protected area. The region exhibits limited topographic variation with elevations ranging from 125 to 195 m. Forest cover is dominated by herb-rich, mesic, and xeric heath forests. The dominant tree species were typical of boreal coniferous forests: Scots pine (*Pinus sylvestris* L.) 48%, Norway spruce (*Picea abies* L.) 29%, and silver birch (*Betula pendula* Roth) and downy birch (*Betula pubescens*

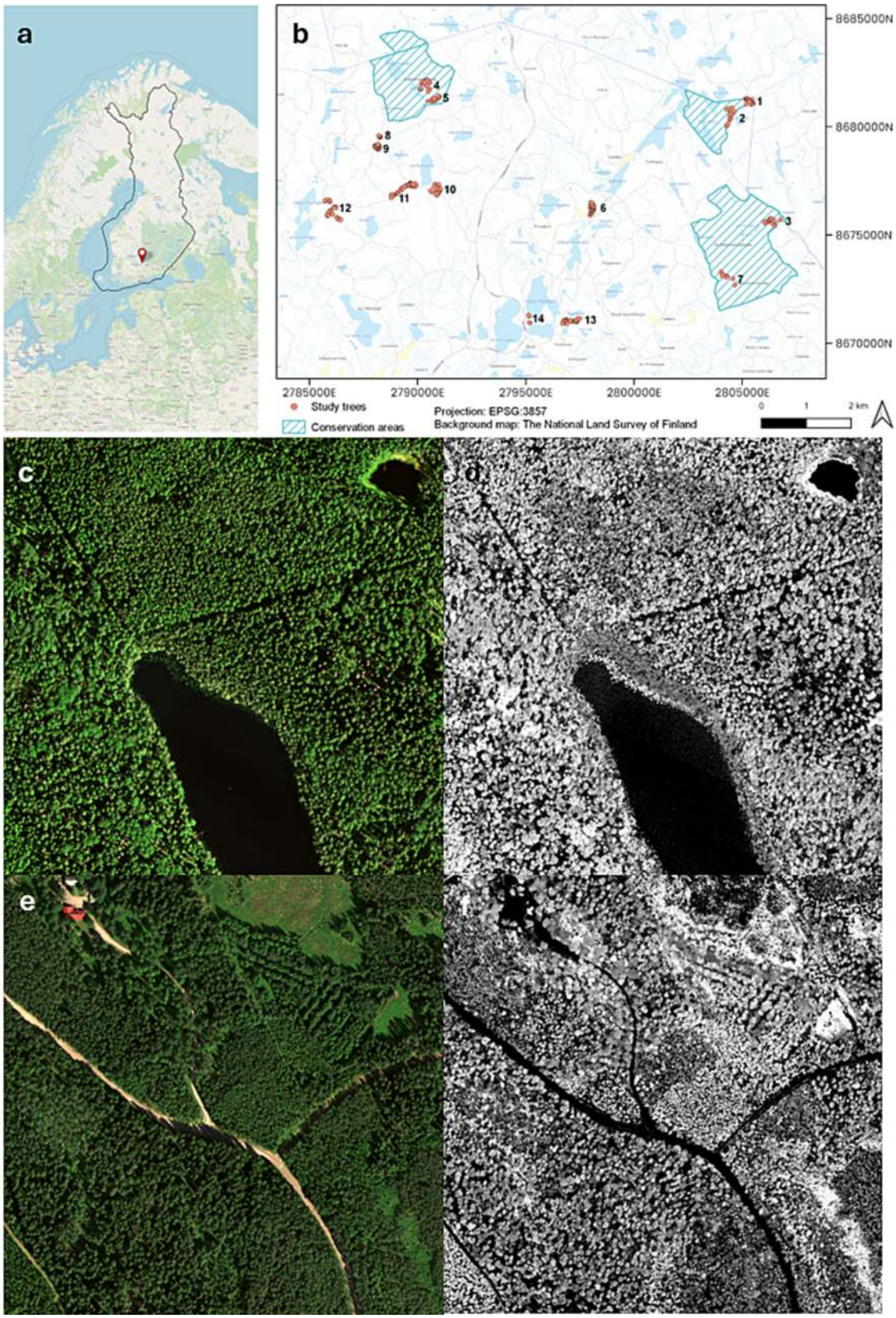



**Fig. 1.** A map of the study area in Southern Finland (a), A detailed map of the 83 km$^2$ study area (1:24,000) showing the sampled aspen trees as dots, sites as a running number and protected zones in raster (b), RGB representation of hyperspectral data (Red: 664 nm, Green: 560 nm, blue: 493 nm) of a protected zone (c) and non-protected zone (e), Normalized difference chlorophyll index image (R1: 598.8 nm, R2: 673.8 nm) of a protected zone (d) and non-protected zone (f). (For interpretation of the references to color in this figure legend, the reader is referred to the web version of this article.)

Ehrh.) 22% of the total basal area. European aspen (*Populus tremula* L.) was patchily distributed and relatively scarce representing 1.4% of the total basal area.

### 2.2. Sampling

Sun-exposed leaves were sampled from the upper crown of 521 individual aspens within the 83 $km^2$ study area. Sampling sites were chosen based on occurrence of aspen. Only aspens with DBH > 10 cm were included in the dataset. No aspens directly next to each other were sampled. The aspens were grouped by zone, with 108, 245 and 168 aspens in protected, non-protected and roadside zones, respectively (Table 1). Sampling from the upper crown minimized self-shading effects, ensuring that all leaves had developed under similar light conditions within the crowns. The main sampling was conducted using throw-line-launchers during 26th June – 5th July 2018. Weather conditions were mostly sunny, with only two days of light rain.

From each tree, four fully expanded leaves with intact petioles were collected. Galled, eaten or pathogen infected leaves were avoided. The leaves were wrapped in aluminum foil to prevent pigment photodegradation, sealed in plastic zipper bags and immediately placed in a cooling box at about 0 °C. Within about 3 h from collection, the samples were frozen in liquid nitrogen (−196 °C) to halt enzymatic activity. Finally, the samples were transported to laboratory in dry ice and stored at −20 °C until analysis.

To evaluate the extent of potential seasonal variation in Chl and Car content during the summer, an additional leaf sampling was conducted on July 17–18, 2018. Here, a subset of 60 aspens (11%) from the main sampling, including all zones, were re-sampled (Suppl. Table 1).

The geographic coordinates of each aspen were recorded using a Topcon HiPer Real-Time Kinematic Global Navigation Satellite System (GNSS, Topcon, Tokyo, Japan). Tree height (m) and the height of the lowest living branches were measured with a Vertex hypsometer (Haglöf Sweden AB, Långsele, Sweden), while diameter at breast height (DBH, cm) was measured using a steel calliper. Crown length (m) was calculated as the difference between total tree height and the height of the lowest living branch. Relative crown length was determined by dividing crown length by total tree height.

### 2.3. Chl and Car content analysis

Pigment content analyses were conducted in a random order under dim light to prevent photodegradation. From each frozen aspen leaf, a 5 mm diameter disc was punched. For each tree, four discs (one per leaf) were punched into two Eppendorf tubes (two discs per tube). The disks were weighed, frozen in liquid nitrogen, and stored at −50 °C until analysis. A pre-cooled stainless-steel bead was added in each tube, and the leaf material was homogenized twice for 30 s using a TissueLyser (Qiagen GmbH, Hilden, Germany), with freezing on dry ice between runs. Samples were extracted in 1.5 ml of pure MeOH using the TissueLyser for 1 min. After centrifugation at 16,900 ×*g* at 4 °C for 5 min, the extraction and centrifugation steps were repeated for the precipitates, and the supernatants combined. Absorbance was measured at 665.2, 652.4, and 470 nm with absorbance at 750 nm for scattering correction, using a UV-1800 spectrophotometer (Shimadzu Corporation, Kyoto, Japan) according to Lichtenthaler and Buschmann (2001) and expressed on a leaf area basis.

**Table 1**
Number of aspen trees (n) in the main sampling and matched tree segments in airborne hyperspectral imagery with outliers excluded, shown separately for protected, non-protected and roadside zones. Coefficients of variation (CoV) for tree and site parameters, separately for protected, non-protected and roadside zones.

| | | Protected | Non-protected | Roadside | Total n |
|---|---|---|---|---|---|
| n (aspens total) | | 108 | 245 | 168 | 521 |
| CoV | Chl content | 0.16 | 0.21 | 0.19 | |
| | Car content | 0.13 | 0.18 | 0.16 | |
| | DBH | 0.34 | 0.35 | 0.37 | |
| | Height | 0.17 | 0.19 | 0.19 | |
| | Crown length | 0.33 | 0.33 | 0.33 | |
| | Relative crown length | 0.22 | 0.23 | 0.23 | |
| n (segmented excluding outliers) | | 65 | 174 | 105 | 344 |
| CoV | Tree density | 0.10 | 0.29 | 0.22 | |
| | Mean height | 0.10 | 0.14 | 0.12 | |
| | Treetop dominance | 0.18 | 0.16 | 0.21 | |

### 2.4. Airborne hyperspectral imagery

HSI and ALS data were collected on a cloudless day during a 2-h and 45-min flight on July 16, 2018, from 08:30 to 11:15, as described in Viinikka et al. (2020). HSI data in the visible and near-infrared (VNIR, 400–1000 nm, bandwidth 3.24 nm) range were collected using HySpex VNIR-1800 camera (Norsk Elektro Optikk AS, NEO, Norway) mounted on a plane. The camera had a field of view of ±8.5 degrees, maximum flight altitude was 1500 m above ground level, and the flight lines overlapped by approximately 23%. The ALS data were collected with Leica ALS70-HP laser scanner (Leica Geosystems, Heerbrugg, Switzerland), resulting in a nominal point density of 8 points per square meter.

Preprocessing of the HSI data, including geo- and orthorectification using Parge 3.4 software (Schläpfer and Richter, 2002), and atmospheric correction using ATCOR-4 software (Richter and Schläpfer, 2002), were performed by the data provider (TerraTec, Norway). The final dataset covered the study area with a spatial resolution of 0.5 m. The ALS point cloud was converted into a canopy height model (CHM) with 0.5 m spatial resolution using TerraScan software (TerraSolid, Helsinki, Finland), as described in Viinikka et al. (2020).

Individual tree crowns were delineated from the CHM using the R package *itcSegment* (Dalponte, 2018; Dalponte et al., 2015). The average spectra for sunlit pixels for each aspen tree were extracted from the crown segments by selecting the top 25% brightest pixels within each crown, following the method of Zarco-Tejada et al. (2002). Noisy spectral range was removed from both ends of the spectrum, resulting in a VNIR range of 432–810 nm. For further details on crown segmentation, see Viinikka et al. (2020) and Mäyrä et al. (2021).

Finally, the field-measured aspens were matched to their corresponding tree segments derived from the canopy height model. Segments of 351 aspens in the HSI data matched the GNSS-located aspens (Table 1). The crown-specific mean spectral reflectance was checked for outliers using principal component analysis (PCA). Seven outliers were excluded from the dataset based on the 97.5% confidence interval of PCA in Simca-P+ (12.1., Umetrics Sartorius).

Site characteristics, i.e. tree density, average tree height, and treetop dominance, were calculated from ALS-derived tree segments within a circular plot of 30 m radius around each aspen. Tree density was defined as the number of trees within the plot. Treetop dominance was calculated as the difference between the height of the measured tree and the average height of all trees within the 30 m radius, with both height values derived from ALS data.

### 2.5. Statistical analysis of the foliar pigment contents, and tree and site characteristics

The comparison of foliar Chl and Car contents, aspen characteristics and site characteristics was tested between protected, non-protected and roadside zones with zone as a fixed factor by 1-way analysis of variance (ANOVA), with Log10 transformed data, except for treetop dominance that was tested with no transformation. Tukey was applied as post hoc test. The comparison of the foliar Chl and Car contents between the main

and additional sampling was performed by repeated measures with sampling date as a repeated factor, and zone and sampling date × zone interaction as fixed factors. The analyses were performed in SPSS (version 27.0.1, IBM SPSS).

Linear regressions between tree and site characteristics were performed for aspen DBH, height, and crown length, for Chl and Car contents, and the relationship of aspen height and relative crown height to tree density were performed separately for protected, non-protected, and roadside zones, with n of 65, 174 and 105, respectively. Linear regressions with Chl content as dependent variable and aspen DBH, height and crown length as the explanatory variable were performed for the aspens of the main sampling, separately for protected, non-protected, and roadside zones, with n of 108, 245 and 168, respectively. Linear regressions with Chl content or Car content as dependent variable and plot characteristics, tree density, mean tree height of all species, and treetop dominance as the explanatory variable were performed separately for protected, non-protected, and roadside zones, with n of 65, 174 and 105, respectively. Regressions of $R^2 > 0.1$ and $p < 0.001$ were considered significant. Regressions were performed in GraphPad Prism 5.

### 2.6. Partial least squares regression with stratified model validation

The relationship between hyperspectral reflectance (432–810 nm) and foliar pigments was modeled using Partial Least Squares Regression (PLSR) in Python using scikit-learn (Pedregosa et al., 2011). To account for the hierarchical and biological structure of the dataset, a stratified grouped-validation framework was implemented. To prevent data leakage, validation was performed at the site level (14 sites), ensuring all samples from a single site were kept together. To ensure biological representativeness, stratification was employed by ecological zone (protected, non-protected, and roadside). This guaranteed that the 70/30 training/test split maintained the same proportion of zones in both sets across 150 random permutations. Within each training iteration, the optimal number of PLS components was selected via 5-fold internal cross-validation (minimizing RMSECV). This rigorous approach ensures that reported performance metrics (mean ± SD) are not dependent on a specific data partition and are representative of all ecological zones.

The non-transformed and transformed datasets of crown specific mean spectral reflectance were compared in ability to predict pigment contents on a leaf area basis by PLSR with mean centering as scaling. The transformations tested included square root, log10, multiplicative scatter correction (MSC), and 1st derivative with Savitzky-Golay smoothing by quadratic fit and window width of 11. Square root and log10 transformed data sets are less skewed and thus less sensitive to saturation effects. MSC is a common spectral transformation in which each spectrum is compared with the mean spectrum and corrected by partial least squares procedure with the aim of correcting light scattering effects and differences in path length (Geladi et al., 1985). The metrics used to evaluate models included coefficients of determination ($R^2$), root mean squared error (RMSE) and relative root mean square error (RMSE% i.e., RMSE/mean of the response variable) to increase the comparability across the response variables.

The variable importance in projection (VIP) was used to show which wavelengths in PLSR model of nontransformed mean spectral reflectance (432–810 nm) had the largest effect (VIP >1) for Chl and Car contents.

Linear regressions with reflectance at 445, 554 and 790 nm as dependent variable and flight time, Chl content, and crown length as the explanatory variable were performed separately for the protected, non-protected and roadside zones to explore possible dependencies within the data. This was done to inspect if the spectral data at specific wavelengths is dependent on flight time and crown length as possible confounding factors, and on Chl content as the target of interest Reflectance wavelengths were chosen as: 445 nm (blue) because it has clear diurnal variation peaking at midday and it does not relate to Chl content (Sims and Gamon, 2002), 554 nm (green hump) because of the relationship to Chl content, and 790 nm (infrared range) because of the dependency on LAI and no relation to Chl content.

### 2.7. Spectral indices and random forest

Training and test sets comprising of 246 (71%) and 99 (29%) aspens, respectively, were randomly generated. To avoid data leakage, all trees of each sampling site were included either in training or test set (Suppl. Table 1). All possible two-band permutations of the 118 wavelength bands between 432 and 810 nm were generated systematically for six different spectral index types for the training set, as in Hoeppner et al. (2020). The index types included simple ratios (SR, eq. 1), normalized difference indices (ND, eq. 2) and some of their modifications. Modified simple ratio mSR_445 (eq. 3) and modified normalized difference mND_445 (eq. 4) include an adjustment in blue (445 nm) to reduce the effect of variation in leaf surface reflectance, chosen since Chl and Car content have minimal effect on reflectance on this wavelength due to saturation (Sims and Gamon, 2002). Modified simple ratio MSR (eq. 5) (Chen, 1996) was suggested as a modification of SR more resistant to geometrical and optical variation within vegetation canopies. Simple ratio of 1st derivative spectrum ($SR_D$, eq. 6) as suggested by Datt (1999) was included in the comparison.

1. $SR = R_{\lambda1} / R_{\lambda2}$
2. $ND = (R_{\lambda1} - R_{\lambda2}) / (R_{\lambda1} + R_{\lambda2})$
3. $mSR_445 = (R_{\lambda1} - R_{445}) / (R_{\lambda2} - R_{445})$
4. $mND_445 = (R_{\lambda1} - R_{\lambda2}) / (R_{\lambda1} + R_{\lambda2} - R_{445})$
5. $MSR = R_{\lambda1} / R_{\lambda2} - (1/[R_{\lambda1} / R_{\lambda2} + 1]^{0.5})$
6. $SR_D = D_{\lambda1} / D_{\lambda2}$

R denotes for reflectance intensity at a given wavelength, and D the value of the 1st derivative spectrum at a given wavelength.

Each spectral index permutation resulted in over 13,800 features, and feeding all of them for further models would have been infeasible. Therefore, we used simple linear regression of the spectral indices to predict Chl and Car contents as the initial variable selection and ranked the most important ones based on their $R^2$-values on the training set. $R^2$-values for each spectral index are shown as heatmaps. From each index set, 50 indices with the highest $R^2$ were chosen to be used as a possible feature set for random forest (RF) along with 118 spectral bands of non-transformed and 1st derivative data. We then trained RFs for each possible input feature combination, resulting in 255 estimators for each target variable. The hyperparameters for each input feature combination were tuned using randomized search with 100 iterations and 3-fold cross validation. Based on the results, we examined for the test set which features correlated with the best predictive performance, and for the best models, which individual features were the most important for each target variable using SHAP (Shapley Additive exPlanations) values (Lundberg et al., 2019; Lundberg and Lee, 2017). In the SHAP plot for Chl and Car content separately, features are ordered according to their importance. The position on the x-axis represents the Shapley value, showing whether the feature has negative or positive effects in the model. The color represents the value of the feature from low to high. Overlapping points are jittered in the y-axis direction to give a sense of the distribution of the Shapley values per feature. Linear regressions were computed using linregress function from scipy (Virtanen et al., 2020), RF analyses were done using scikit-learn (Pedregosa et al., 2011), and SHAP values were derived using shap Python library.

## 3. Results

### 3.1. Variation in pigment contents and aspen characteristics

There was a large variation among aspen trees in foliar Chl and Car contents on a leaf area basis (Fig. 2a, b, Suppl. Fig. 1, Table 1).

Coefficients of variation were 0.16–0.21for Chl and Car content, respectively, with the highest coefficient of variation in non-protected zone. Aspens in protected zone had slightly higher foliar Chl and Car content than those in non-protected zone, with roadside zone differing from neither (Fig. 2a,b, Table 2). The Chl content of individual aspens increased during the summer (Suppl. Fig. 2, Suppl. Table 2), whereas Car content did not change between the samplings (Suppl. Table 2).

Aspens in protected zone were thicker and taller than in non-protected zone (Fig. 2c,d, Table 2). The thickest and tallest aspens were found in old growth forest in Kotinen conservation area (Suppl. Fig. 3). Aspens differed among protected, non-protected and roadside zones in crown length and relative crown length (Fig. 2e,f, Table 2), Crown was longer in roadside than in non-protected zone, and as relative crown length also longer in non-protected than in protected zone. Tree density was higher in non-protected than in protected or roadside zones (Fig. 2g). Mean tree height (of all species) was the highest in protected zone and the lowest in non-protected zone (Fig. 2h, Table 2). Treetop dominance status of the measured aspen did not differ among zones (Fig. 2i).

The relationship of tree height to DBH to was strong ($R^2$ 0.33–0.4) with similar slope across landscape (Fig. 3a). The relationship of crown length to DBH and had a stronger $R^2$ (0.41–0.48) with a steeper slope in non-protected and roadside zones than in protected zones ($R^2$ 0.34), the latter having shorter crown lengths (Fig. 3b). The relationship of crown length to tree height had stronger $R^2$ in protected zones (0.65) in non-protected and roadside zones (0.51–0.53) with a s similar slope but lower values for the intercept (Fig. 3c). The relationship of relative crown length to tree height had significant $R^2$ only in protected zone (Fig. 3d). There was a weak tendency of higher relative crown length with a lower density of trees in non-protected and roadside zones, but no association in protected zone (Fig. 3e). Higher density of trees was related to lower mean height across all tree species, but only in protected zone (Fig. 3f). The relation between Chl and Car contents was strong and highly similar across landscape (Suppl. Fig. 4).

**Table 2**
Differences in chlorophyll content (Chl), carotenoid content (Car), aspen characteristics, and site characteristics (including all tree species) among the protected, non-protected and roadside zones tested by one-way Anova.

| Parameter | F | *p* |
|---|---|---|
| Chl | 4.6 | **0.011** |
| Car | 6.2 | **0.002** |
| DBH | 49.8 | **<0.001** |
| Tree height | 44.5 | **<0.001** |
| Crown length | 4.4 | **0.013** |
| Relative crown length | 36.4 | **<0.001** |
| Tree density | 72.2 | **<0.001** |
| Tree mean height | 42.4 | **<0.001** |
| Treetop dominance | 1.3 | ns |

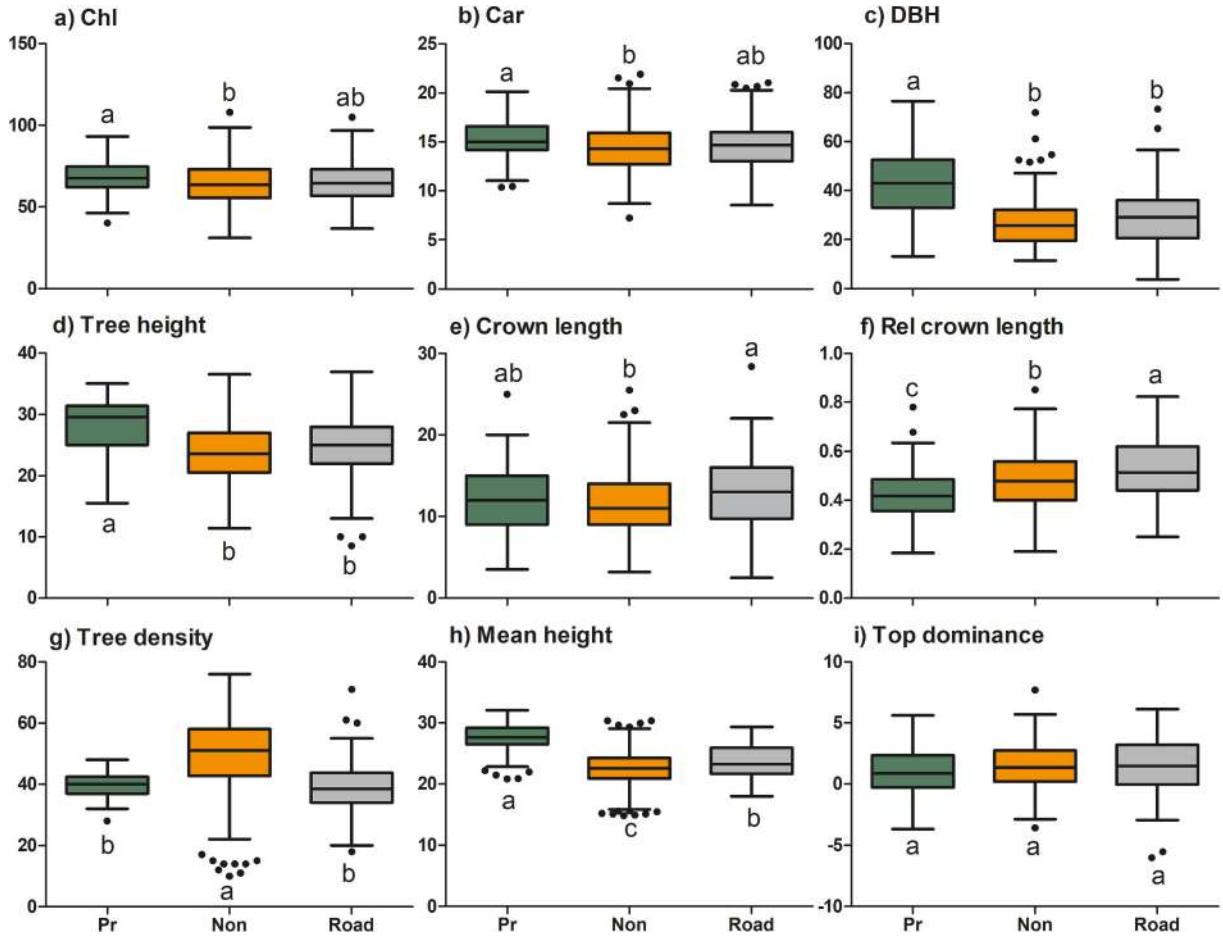



**Fig. 2.** Foliar a) chlorophyll content (Chl, μg $cm^{-2}$), b) carotenoid content (Car, μg $cm^{-2}$), c) diameter at breast height (DBH, cm), d) height (m), e) crown length (m) and f) relative crown length (m), g) tree density, h) mean tree height (m) and i) treetop dominance, across protected (Pr), non-protected (Non) and roadside (Road) (<25 m distance from road) zones. (a-f) represent aspen characteristics, whereas (g-i) represent site characteristics across all tree species. Boxplot depicts median and quartiles, with whiskers denoting Tukey test grouping, jittered points showing outliers. Alphabets indicate differences among zones.

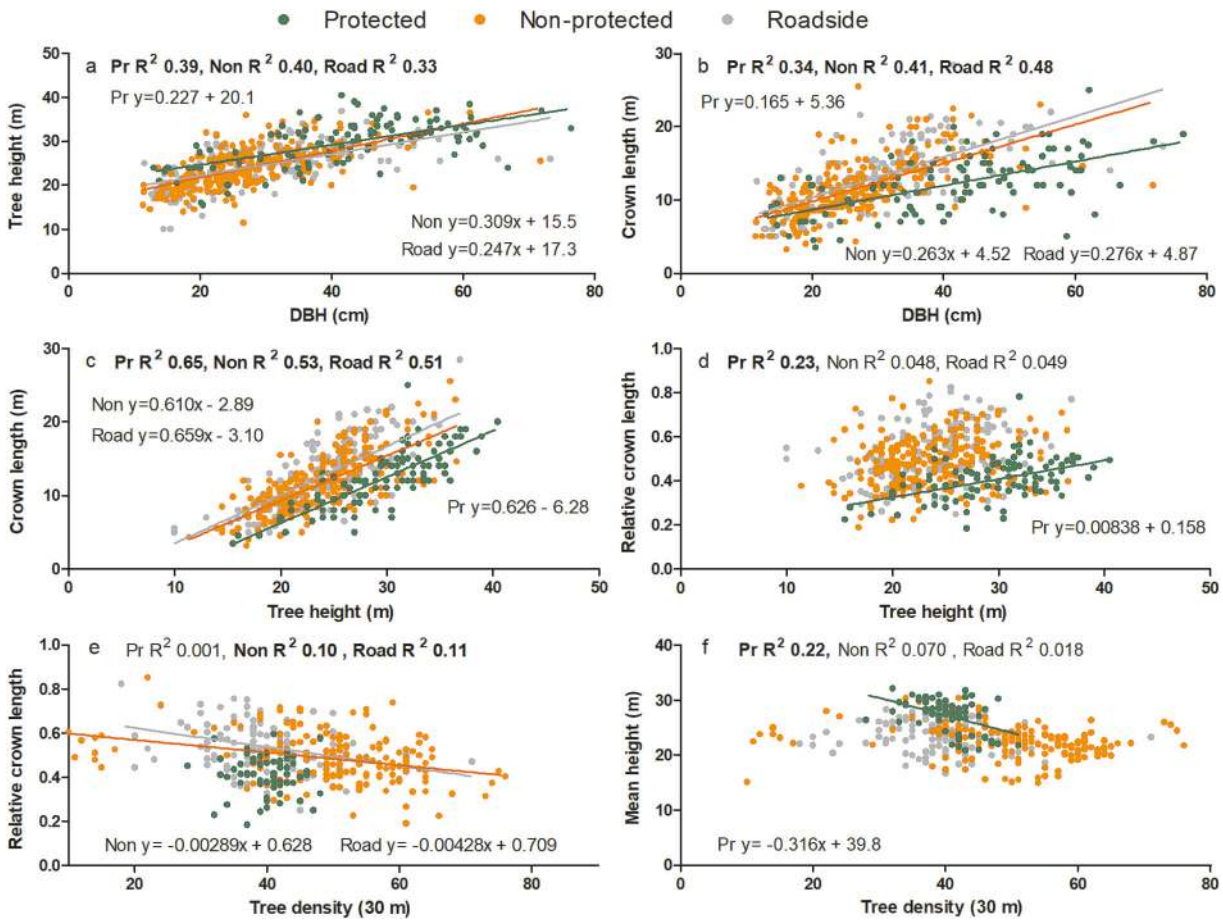



**Fig. 3.** European aspen characteristics showing the relations between a) tree height and DBH, b) crown length and DBH, c) crown length and tree height, d) relative crown length and tree heigh, e) relative crown height and forest tree density in a 30 m radius circular plot, and f) tree mean height across tree species and stand tree density. Color scheme by zone with protected as green, non-protected as orange and roadside (<25 m to the road) as gray. Relations of $R^2 > 0.1$ and $p < 0.001$ are shown in bold, with regression line and equation. (For interpretation of the references to color in this figure legend, the reader is referred to the web version of this article.)

### *3.2. Tree and site characteristics influenced pigment contents in non-protected forests and roadsides*

In non-protected and roadside zones, aspens with a larger DBH had a higher foliar Chl content (on an area basis, μg/cm$^2$) (Fig. 4a). There was no significant relation between Chl and aspen height (Fig. 4b), whereas aspens with longer relative crown length had higher Chl content in non-protected forests (Fig. 4c). In non-protected and roadside zones, foliar Chl content of aspen had an inverse relationship with the density of neighboring trees with trees at the densest sites having the lowest foliar Chl content (Figs. 2, 4d). By contrast, in protected zone sites, Chl content had no clear association with tree density or any other tree characteristics (Fig. 4a,b,c,d). A higher foliar Chl content, however, tended to co-occur with higher mean tree height (of all species) in protected forests (Fig. 4e). There was no significant relation between foliar Chl content and top dominance of the measured aspen (Fig. 4f).

Car content was negatively associated with tree density in non-protected and roadside zones with high Car content in low tree density (Fig. 5). There was no significant relation between Car content and any other tree or site characteristics (Suppl. Fig. 5).

### *3.3. Accuracy assessment of pigment content estimation by PLSR*

Accuracy of Chl content estimation had $R^2$ 0.51 and RMSE 13.4% by PLSR (Table 3). For Car content, the accuracy was lower ($R^2$ 0.32 and RMSE% 13.5 (Table 3). There was a high similarity of the influential wavelength ranges for Chl and Car contents. The most influential wavelengths for Chl content in the best-performing PLSR model were the green hump (525–579 nm), 670–680 nm, the red edge (698–715 nm) and NIR range (745–810 nm) and for Car content 520–575 nm, 660–689 nm, 698–715 nm and 745–810 nm (Fig. 6).

Aspen-crown specific mean spectral reflectance was positively related to flight time in the blue (445 nm), in the green (540 nm) and in NIR (790 nm) range, but relationship was strongest in the blue range (Suppl. Fig. 6a,b,c). Chl content had no relation to reflectance in the blue or NIR, but a negative relation to reflectance in the green range (554 nm) in the protected zone (Suppl. Fig. 6e). Crown length had a positive relation to reflectance in the blue and NIR range (Suppl. Fig. 6 g, i), but

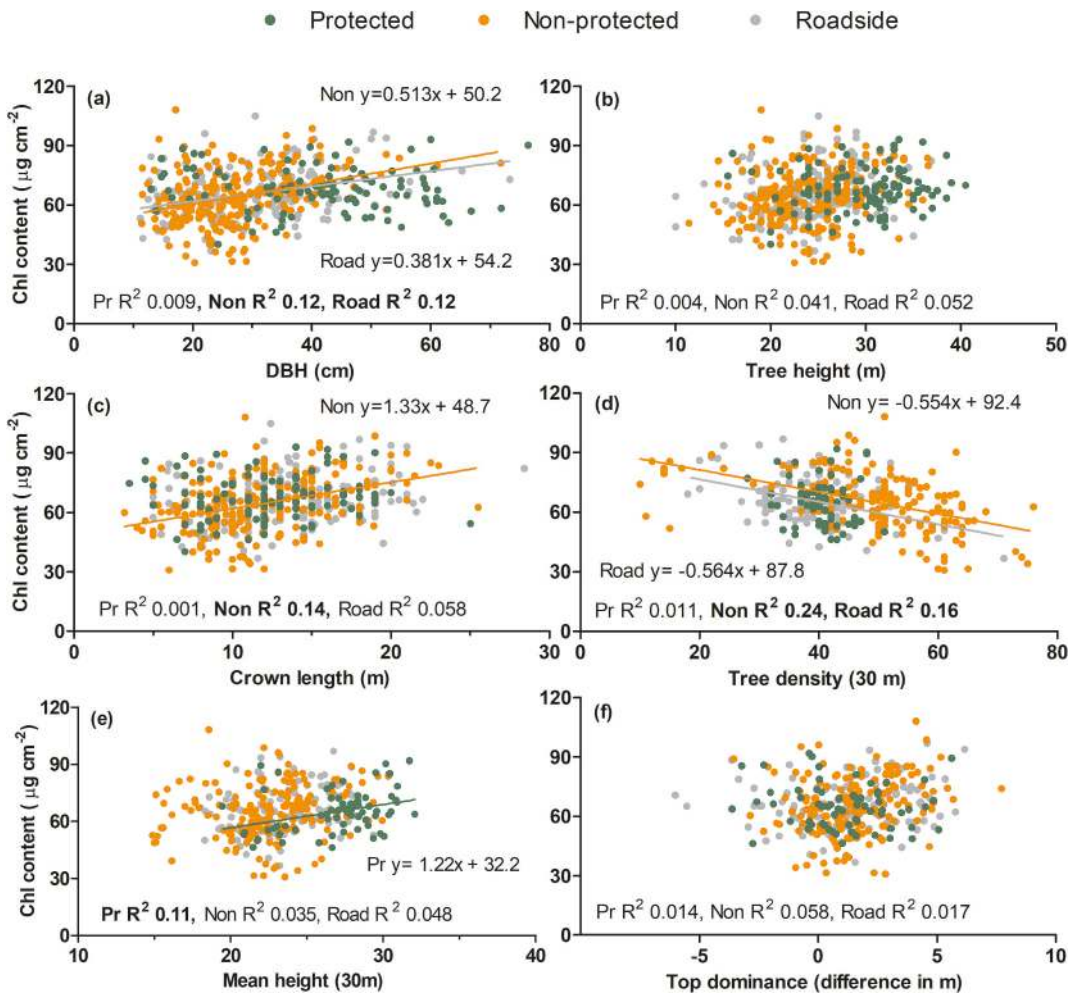



**Fig. 4.** Regression of chlorophyll (Chl) content (µg $cm^{-2}$) with a) DBH, b) tree height, c) crown length of aspens, and (d) tree density (number of trees in a 30 m radius circular plot), e) average tree height in a 30 m radius circular plot and (f) treetop dominance. (a-c) aspen characteristics, (d-f) site characteristics across all tree species. Color scheme by zone with protected as green, non-protected as orange and roadside (< 25 m from road) as gray. Relationships of $R^2 > 0.1$ and $p < 0.001$ are shown in bold, with regression line and equation. (For interpretation of the references to color in this figure legend, the reader is referred to the web version of this article.)

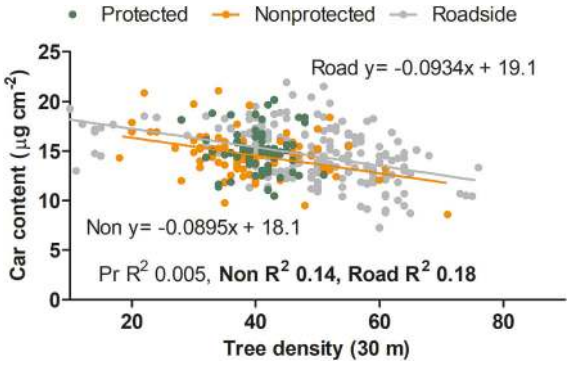



**Fig. 5.** Regression of Car content (µg $cm^{-2}$) with tree density (number of trees in a 30 m radius circular plot). Color scheme by zone with protected as green, non-protected as orange and roadside (< 25 m from road) as gray. Relations of $R^2 > 0.1$ and $p < 0.001$ are shown in bold, with regression line and equation. (For interpretation of the references to color in this figure legend, the reader is referred to the web version of this article.)

**Table 3**
Comparison of partial least squares regression (PLSR) models with non-transformed and transformed HSI (432–810 nm) data sets for estimations of chlorophyll (Chl) and carotenoid (Car) contents. n number of factors in the model, $R^2$ coefficient of determination, RMSE root mean square error, RMSE% relative root mean square error (mean ± standard deviation across 150 stratified iterations). Transformations included square root (sqrt), logarithm base 10 (log10), multiplicative scatter correction (MSC) and 1st derivative (1st D) for spectral reflectance. All models were made with mean centering (Ctr). Best values and models bolded.

| Target | Model | n | $R^2$ | RMSE | % RMSE |
|---|---|---|---|---|---|
| Chl content | **Non** | **5.69 ± 1.95** | **0.51 ± 0.09** | **8.77 ± 0.37** | **13.43** |
| | Sqrt | 5.25 ± 1.8 | 0.51 ± 0.09 | 8.77 ± 0.34 | 13.43 |
| | Log10 | 4.93 ± 1.66 | 0.50 ± 0.1 | 8.81 ± 0.33 | 13.49 |
| | MSC Ctr | 4.40 ± 1.42 | 0.43 ± 0.1 | 9.32 ± 0.43 | 14.27 |
| | 1st D Ctr | 5.69 ± 1.82 | 0.50 ± 0.08 | 8.89 ± 0.41 | 13.61 |
| Car content | **Non Ctr** | **5.35 ± 1.84** | **0.32 ± 0.11** | **1.98 ± 0.07** | **13.47** |
| | Sqrt Ctr | 5.18 ± 1.8 | 0.31 ± 0.11 | 1.98 ± 0.07 | 13.47 |
| | Log10 Ctr | 4.77 ± 1.53 | 0.30 ± 0.12 | 1.99 ± 0.07 | 13.54 |
| | MSC Ctr | 3.19 ± 0.62 | 0.27 ± 0.11 | 2.02 ± 0.07 | 13.74 |
| | 1st D Ctr | 4.58 ± 1.93 | 0.28 ± 0.12 | 2.02 ± 0.07 | 13.74 |

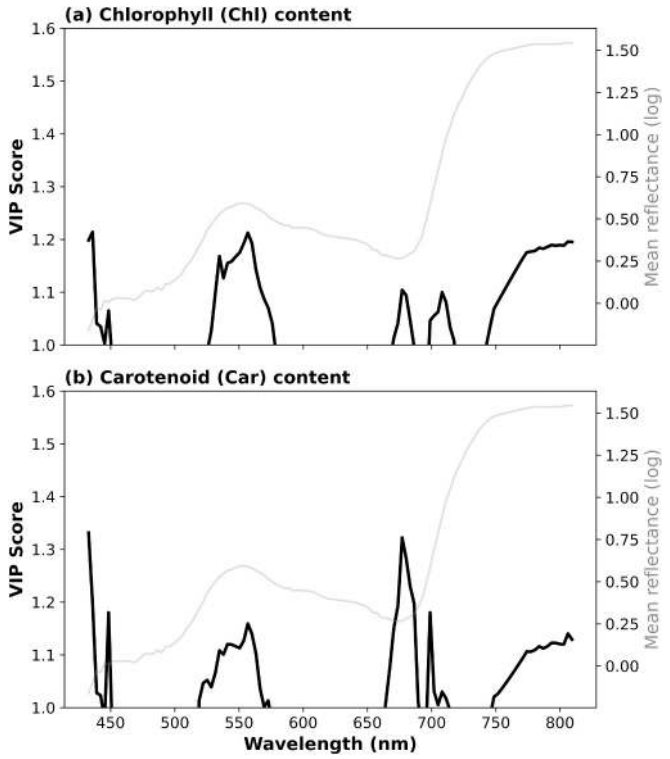



**Fig. 6.** The variable importance in projection (VIP) of wavelengths in PLSR model of mean spectral reflectance (432–810 nm) for (a) chlorophyll (Chl) and (b) carotenoid (Car) content. Y-axis was cut at 1 since values >1 denote above average importance. Mean spectral reflectance with gray line on the background, with right y-axis.

**Table 4**
The best performing random forest models for Chl and Car content.

a) Chl content

| Feature set | $R^2$ | RMSE | RMSE% |
|---|---|---|---|
| ND, mSR_445, mND_445 | 0.522 | 7.579 | 11.73 |
| SRI, mSR_445, mND_445 | 0.518 | 7.578 | 11.77 |
| Reflectance data, MSR, mSR_445, mND_445 | 0.515 | 7.601 | 11.81 |
| MSR, mSR_445, mND_445 | 0.514 | 7.613 | 11.83 |
| Reflectance data, ND, mSR_445, mND_445 | 0.512 | 7.626 | 11.85 |
| Reflectance data, SRI, mSR_445, mND_445 | 0.511 | 7.632 | 11.86 |
| Reflectance data, MSR, mND_445 | 0.510 | 7.639 | 11.87 |
| ND, mND_445 | 0.510 | 7.641 | 11.88 |
| SRI, mND_445 | 0.509 | 7.647 | 11.89 |
| ND, mSR_445 | 0.509 | 7.651 | 11.89 |

b) Car content

| Feature set | $R^2$ | RMSE | RMSE% |
|---|---|---|---|
| Reflectance data, ND, mSR_445 | 0.284 | 1.915 | 13.23 |
| Reflectance data, ND, mSR_445, mND_445 | 0.282 | 1.918 | 13.25 |
| Reflectance data, ND, mND_445 | 0.280 | 1.919 | 13.26 |
| Reflectance data, MSR, mSR_445, mND_445 | 0.277 | 1.924 | 13.29 |
| Reflectance data, derivative data, MSR, mSR_445 | 0.275 | 1.927 | 13.31 |
| Reflectance data, derivative data, SRI, mND_445 | 0.274 | 1.928 | 13.32 |
| ND, mSR_445, mND_445 | 0.272 | 1.930 | 13.33 |
| Reflectance data, SRI, mSR_445 | 0.272 | 1.930 | 13.34 |
| Reflectance data, derivative data, ND, MSR, mSR_445, mND_445 | 0.271 | 1.932 | 13.35 |
| Reflectance data, derivative data, ND, SRI, mSR_445, mND_445 | 0.271 | 1.932 | 13.35 |

no relation in the green range (Suppl. Fig. 6 h).

### 3.4. Pigment content estimation by indices

Based on the linear regression analyses of all possible wavelength combinations for the six index types, the simple ratios of 1st derivative reflectance data ($SR_D$) had the highest $R^2$ for Chl and Car contents in the training set (Suppl. Figs. 7, 8, Suppl. Table 4). The wavelengths resulting in the highest coefficients of determination were highly similar for the two pigments (Table 4, Suppl. Figs. 7, 8).

The most frequent spectral index types to yield high predictive performance for Chl and Car content in a combination of two or more indices were mND_445 and mSR_445 (Table 4). The best performing RF models for Chl content estimation contained mND_445 as their input feature. The best spectral index combination for Chl content was ND, mSR_445 and mNR_445, achieving test $R^2$ of 0.52 and RMSE% of 11.7 (Table 4). According to SHAP values, the most important individual

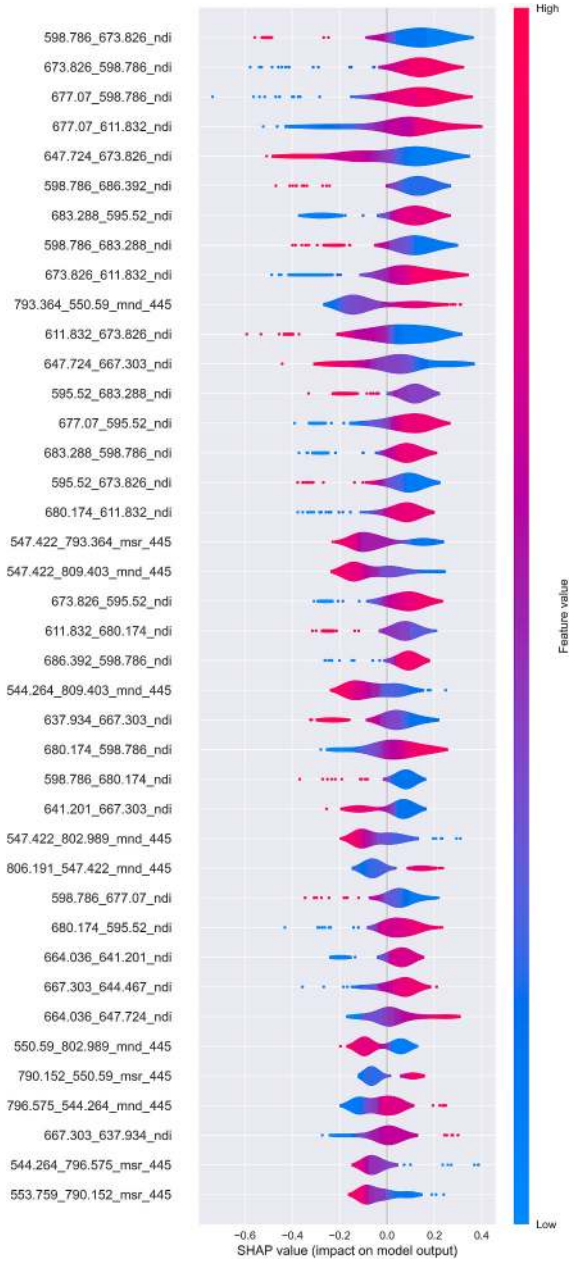



**Fig. 7.** SHAP results of random forest model with best 40 indices for Chl content in test set.

input features for the best performing model were ND for wavelengths with one band between 598 nm and 612 nm, and the other band between 667 nm and 686 nm (Fig. 7). With mND_445 and mSR_445 the most influential wavelengths were different than with ND, 555 nm and 793 nm (Fig. 7). Overall, SHAP analysis considered ND to be more important than mND_445 or mSR_445, despite mND_445 being more frequently included in the best performing models.

The predictive performance of RF models for Car content was lower than for Chl content, as the best model achieved $R^2$ score of 0.283 and RMSE% of 13.2 for the test set. For these data also, the input features corresponding to higher predictive performance were mND_445 and mSR_445. However, the best feature set for Car content contained the non-transformed reflectance data, ND and mSR_445 (Table 4). SHAP values for the best performing model indicated that ND with wavelengths between 588 nm and 615 nm as one band and between 667 and 683 nm as the other band influenced the predictions the most (Fig. 8).

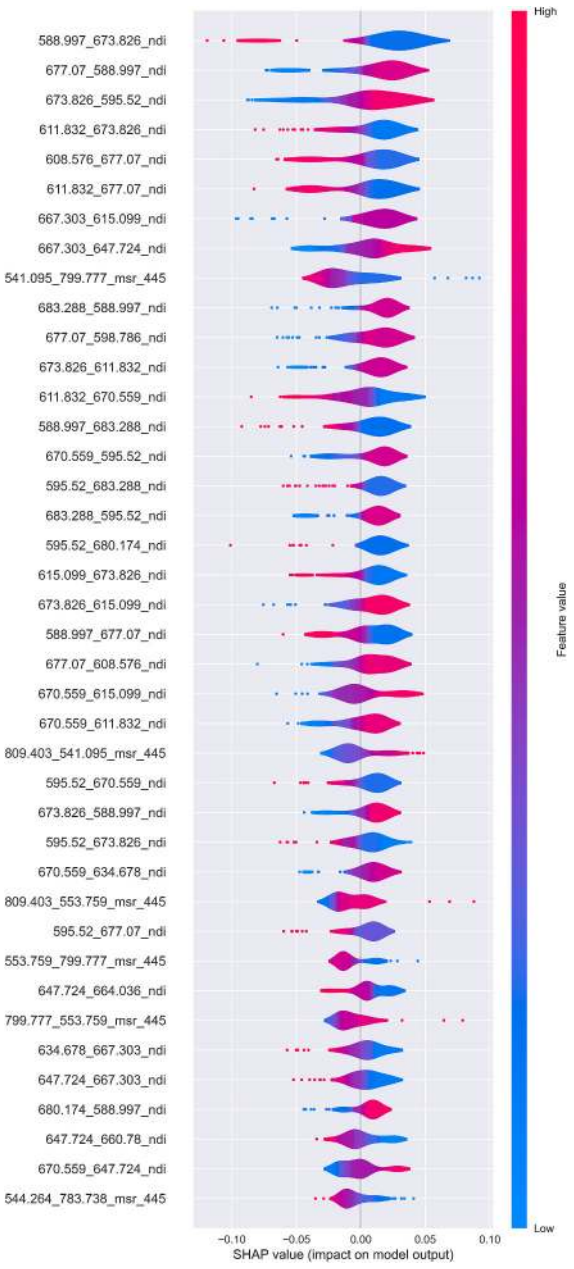



**Fig. 8.** SHAP results of random forest model with best 40 indices for Chl content in test set.

## 4. Discussion

### 4.1. Intraspecific diversity in pigment contents

Aspen trees had a high variation in average Chl and Car pigment contents in the upper crowns across the landscape. This may be due to 1) genetic differences (Madritch et al., 2014), 2) variation in plant health and vigor (Croft et al., 2017; Croft and Chen, 2018; Nestola et al., 2018), 3) edaphic factors such as soil nutrient content (Esteban et al., 2015) and (4) light conditions (Lichtenthaler et al., 2007). Large differences in spectral reflectance among genotypes have previously been shown for quaking aspen that forms large clonally reproducing monospecies forests (Madritch et al., 2014). In contrast, European aspen can mostly occur in genets of a single ramet (Suvanto and Latva-Karjanmaa, 2005). Therefore, for European aspen genotypes having a similar variation among genotypes compared to quaking aspen, the genotypic differences occur on a considerably smaller spatial scale. Thus, European aspen has a great potential for high genotypic differences within a landscape. High intraspecific diversity of aspen Chl and Car contents can contribute to diversity of forage quality for the variety of herbivores that utilize aspen as a food source, and for decomposers such as polypores. This may support the high biodiversity that aspen is able to account for.

The CoVs for were 0.16–0.21 and 0.13–0.18 across zones for Chl and Car content, respectively. While these were smaller than for morphological plant traits such as DBH and aspen height, it can be considered high as intraspecific variation for strictly controlled primary metabolites. Li et al. (2018b) found CoV for Chl content to be 0.4 when interspecific variation was included. The proportion of intraspecific variation to total variation in Chl content has been studied for few tree species, and it has been up to 51% for a temperate forest area with environmental gradients (Spasojevic et al., 2016), 14.5% for Australian forest biomes (Chiarenza et al., 2024) and less than 20% in a north to south forest transect in eastern China (Li et al., 2018a, 2018b).

The slightly higher Chl and Car contents in protected zone than in non-protected one is unexpected if one considers the higher average age of the aspens in protected area. If a high foliar Chl content is interpreted as an indicator of plant health (Croft et al., 2017; Croft and Chen, 2018), the result indicates that old aspens of protected forest can have slightly higher vigor and photosynthetic capacity than the ones in managed forest. This is contrary to the common thinking that all old trees would have lower photosynthetic capacity than younger ones, even though it has mostly been shown for coniferous tree species (Bond, 2000). The slightly higher Chl content in protected areas can be related to higher trees having higher Chl content on a leaf area basis.

### 4.2. Tree and site characteristics and their influence on pigment contents

The aspens in protected zone were generally thicker and taller than in non-protected and roadside zones. As a rule, thicker and taller aspens had a longer crown, but the increase in crown length with increased DBH was much steeper in non-protected forests and roadsides than in protected forests. The shorter crown length of protected forests was probably due to light conditions with shading by higher canopy trees and older tree age in pristine old growth forests than in managed forests. Short crown length of aspen increases the number of stratified canopy layers within old growth forest. With increasing aspen age, the crown tends to lengthen until age of 20 or 25 years (Kull and Tulva, 2000; Lieffers et al., 2002), and after that the crown shortens as the aspen ages. Thus, leaf area index, LAI, i.e. one-sided green leaf area on a unit ground surface area, decreases with increasing aspen age (Lieffers et al., 2002), which agrees with shorter crown length in protected zone of this study.

The thickest aspens had a higher Chl content than thinner ones and the lowest Chl content (μg $cm^{-2}$) co-occurred with highest tree density in non-protected and roadside zones. The result implies that light conditions affect foliar Chl content, since neighboring trees shade each other especially in dense forest areas. Light availability affects Chl and

Car contents on a leaf area basis so that pigment content is higher or similar in sun-leaves than in shade-leaves, depending on tree species (Evans and Poorter, 2001; Lichtenthaler et al., 2007; Rozendaal et al., 2006). In this study, all sampled leaves were sun leaves but some difference in their light environments can be assumed since increased shading can be expected with increasing tree density. The lack of relation between Chl content and tree density in protected areas was likely due to a narrow distribution of tree density values in them.

Dense managed patches may be due to delayed thinning, whereas low density patches were under strong human influence in non-protected and roadsides zones. The old-growth sites were more uniform in light conditions with no high-density patches. This may be due to aspen establishment history since aspen is a light-dependent species that needs disturbance, such as fire, for establishment (Lankia et al., 2012; Linder et al., 1997). Recruitment of young aspens is the critical step for aspen renewal (Hardenbol et al., 2020), which can thus lead to rather even-aged cohorts (Lankia et al., 2012). In another protected area in Finland, majority (93%) of the mature aspens was over 150 years old, and probably established after fire events of human influence, particularly slash-and-burn cultivation and pasture burning (Lankia et al., 2012). The light conditions can be expected to vary more between non-protected sites depending on time after clearcut or thinning than in protected zones. Ideally, one would acquire measurements of light intensity or LAI near the positions of leaf samples collected to prove light intensity differences. Unfortunately, we did not implement this, and it is acknowledged as a limitation of this study. However, Chl content of aspen leaves had a stronger association with tree density than with top dominance. This is in accordance with the expected differences in light availability, particularly for diffused light within the forest canopy. Distance to neighboring trees can thus affect the radiation received by a tree more than height differences (top dominance) of the trees (Li et al., 2023).

### 4.3. Pigment content estimation by HSI

Airborne hyperspectral data together with ALS enabled the estimation of foliar Chl and Car contents for individual tree crowns. The goodness of fit for Chl estimation in this study was moderate, slightly higher for the index-based RF approach than the PLSR model. The low standard deviations across 150 iterations indicated high model stability when ecological zones were proportionally represented. Notably, the inclusion of zone stratification improved predictive performance, suggesting that the model successfully captured spectral-chemical relationships consistent across different zones. A combination of HSI and ALS has been utilized by others to show high accuracies for Chl content estimation. Asner et al. (2015) showed $R^2$ of 0.7 and RMSE% of 15.6 for a wide range of tropical tree species. Lin et al. (2019) showed $R^2$ of 0.89 and RMSE of 6.03 for Chl content modelling for Yunnan pine in a forest area with damage by pine shoot beetles and thus partly very low Chl content and thus wide dynamic range for estimation. This can be interpreted as high overall health of aspen foliage in this study.

The green hump and red edge range were the most influential wavelengths for Chl content estimation by PLSR model. Red edge range has commonly been the most influential range for Chl estimation (Croft et al., 2014; Tsuchiya et al., 2025). The overall best accuracies were achieved by combinations of ratios including ND, mSR_445 and mND_445 for Chl content. The reflectance in the blue range (445 nm) was originally suggested by Sims and Gamon (2002) as a measure of surface reflectance. Here we showed that reflectance at 445 nm was affected by the flight time during the mission. The change in reflectance at 445 nm was a good approximation of the change in light quality and intensity during the morning. Early morning sunlight has less blue light than later during the day since short wavelengths scatter more when the sun is low and light travels a longer distance through the atmosphere. Thus, the change in reflectance in the blue helped to adjust for the light quality change during the morning. Since reflectance at 445 also correlated with crown length, indices mSR_445 and mND_445 may be less affected by variation due to two separate confounding factors: sunlight quality and LAI effect. This improved the performance of the pigment content estimations in this study, as seen in the good performance of mSR_445 and mND_445 for Chl retrieval. The overall most influential features for Chl estimation in SHAP analysis were normalized difference indices utilizing the maximum absorbance features (664–686 nm) of Chl, together with 598–662 nm), which implies that Chl content levels were not high enough to saturate the model.

The low overall estimation accuracy for Car content was probably due to overlapping absorbance range with Chl content and higher content of Chl than carotenoids, as previously proposed (Blackburn, 1998), and in this study, indirect relationship to the best indices. The similarity of the best indices for Car and Chl content estimation was likely due to the strong relationship between the pigment contents. Thus, in this study, the best indices for Car content estimation were the ones that estimate Chl content and only indirectly are related to Car content because of their strong relationship. Strong relation between Chl and Car contents can be expected for healthy plants, whereas in stressed plants Chl/Car ratio decreases due to Chl content being negatively affected by stress more strongly than Car content (Chen et al., 2022; He et al., 2023). This can be interpreted as an indication of high vigor of aspen foliage in the middle of the growing season in protected forests as well as non-protected and roadside zones.

### 4.4. Ecological implications of this study

A keystone species is important for the whole ecosystem functioning, and conservation of habitats of keystone species has been suggested as an efficient “mega-conservation” strategy, to preserve the wide array of species diversity associated with or dependent on them (Rogers et al., 2020). In this study, we showed aspens in protected areas to differ from those in managed forest with high foliar Chl content in the upper crown, thicker stem and shorter crown length. The relations of Chl content to tree characteristics differed between protected and non-protected forests implying the special nature of large aspens in protected zone. The ecological significance of large trees is well-known since large trees allow for a high diversity of microhabitats that serve for a higher biodiversity (Paillet et al., 2017). The overall volume of standing trees in old-growth forests is often larger than in managed forests, which can also lead to a larger carbon stock in old-growth forests than in managed forests (Akujärvi et al., 2026).

The roadside zone was included in this study since roadsides represent a notable proportion of suitable living environment for aspen in Finland. In non-protected areas, majority of aspens grow on roadsides, whereas in protected areas majority of aspens grow in the old forest (Mäyrä et al., 2021; Palmroos et al., 2023). The basal area of 1.4% for aspen in a study area rich of old forests (Mäyrä et al., 2021) can be considered alarmingly low, since aspen tends to decline in old-growth forests due to low recruitment (Hardenbol et al., 2020; Lankia et al., 2012; Latva-Karjanmaa et al., 2007). Aspen has been shown to recruit on roadside forest edges, but not inside old forests (Hardenbol et al., 2020).

Chl content has been suggested as a remote sensing-based biodiversity indicator (Skidmore et al., 2021). Generally, Chl content is higher in the leaves of deciduous trees than in the needles of the coniferous trees, both on a leaf area basis and on mass basis (Li et al., 2018b; Minocha et al., 2009). Thus, due to high biodiversity in deciduous forests, high biodiversity could co-occur with high Chl content. However, because of differences in Chl content among plant species (Li et al., 2018b) and light availability affecting the intraspecific variation in plant Chl content, overall, the relationship of Chl content to biodiversity cannot be a straightforward one. Also in this study, both the highest and lowest stand-level average Chl contents occurred in non-protected zone with light availability probably contributing to the observed variation.

There is a need for efficient use of remote sensing in monitoring of

biodiversity, ecosystem structure, and ecosystem functioning (Cavender-Bares et al., 2022). For a wide-range assessment of ecological indicators, utilization of satellite scale data would be ideal in terms of spatial and temporal coverage. Thus far, Chl content has been estimated and mapped using, e.g., Landsat 5 TM canopy reflectance (Croft et al., 2020). Next generation satellite scale hyperspectral imaging (e.g., CHIME, SBG) will increase the possibility of high accuracy estimations when it becomes available. This will allow for large-scale monitoring of intraspecific variation in physiological traits.

### 4.5. Conclusions

This study adds to the limited knowledge of pigment contents in the upper crowns of old growth forests and showcases the differences in aspen structural characteristics between old and managed forests. Pigment contents of a keystone species, European aspen, have high diversity on landscape level, which may in turn contribute to the overall diversity of forage quality of aspen for herbivores and decomposers. Diversity of resource quality can result in an increase in biodiversity that can cascade throughout the forest community. The density of neighboring trees can influence Chl and Car content, as was shown in this study for non-protected forest and roadside zones, where aspens with the highest Chl contents co-occurred with the lowest tree densities. Leaf Chl content was estimated by combining HSI and ALS for single crowns of a keynote species with good accuracy. We also show that reflectance at 445 nm was affected by both tree crown length and the light availability during the flight mission. Thus, the modified indices adjusted with reflectance at 445 nm can be useful in a combined correction of light conditions and leaf area index for improved aspen pigment content estimation using airborne hyperspectral imaging data.

## CRediT authorship contribution statement

**Sarita Keski-Saari:** Writing – original draft, Visualization, Validation, Methodology, Investigation, Formal analysis, Conceptualization. **Markku Keinänen:** Writing – review & editing, Methodology, Conceptualization. **Janne Mäyrä:** Writing – review & editing, Visualization, Software, Methodology, Formal analysis. **Arto Viinikka:** Writing – review & editing, Software, Investigation, Data curation. **Topi Tanhuanpää:** Writing – review & editing, Investigation. **Sonja Kivinen:** Writing – review & editing, Investigation. **Laura Poikolainen:** Writing – review & editing, Investigation. **Ehsan Khoramshahi:** Formal analysis, Writing – review & editing. **Petteri Vihervaara:** Writing – review & editing, Funding acquisition, Conceptualization. **Timo Kumpula:** Writing – review & editing, Project administration, Funding acquisition, Conceptualization.

## Funding

The research was funded by the Strategic Research Council under the Academy of Finland (IBC-Carbon, project numbers 312636, 335959), the Research council of Finland (C-NEUT, project number 347862) and the Finnish Ministry of the Environment (Finnish Ecosystem Observatory project number VN/12351/2021-YM-2). MK was supported by Research Council of Finland Flagship Programme, Photonics Research and Innovation (PREIN), decision 346518.

## Declaration of competing interest

The authors declare that they have no known competing financial interests or personal relationships that could have appeared to influence the work reported in this paper.

## Acknowledgements

We thank the anonymous reviewers for their valuable comments that helped to improve the manuscript, Sinikka Sorsa for her help in chemical analysis, Franziska Wolff for insightful comments, and Elina Koivisto, Aleksi Ritakallio, Pasi Korpelainen, Anton Kuzmin, Max Strandén, Franziska Wolff, Niina Kiljunen, Xi Zhu, and Aleksandra Riki for their contribution in the field work.

## Appendix A. Supplementary data

Supplementary data to this article can be found online at https://doi.org/10.1016/j.ecoinf.2026.103863.

## Data availability

Data is publicly available through Geoportti.
https://geoportal.uef.fi/PublicProjectView/35
Code is available at:
PLSR: https://geoportal.uef.fi/PublicProjectView/35
RF: https://github.com/mayrajeo/aspen_hyperspectral

## References

Akujärvi, A., Nirhamo, A., Heikkinen, R.K., Pykälä, J., Saikkonen, O., Green, T., Peltoniemi, M., Mäkelä, A., 2026. The relationship between tree carbon dynamics and the occurrences of epiphytes of conservation concern in boreal unmanaged forests. Eur. J. Forest Res. 145, 30. https://doi.org/10.1007/s10342-025-01867-1.

Alonzo, M., Bookhagen, B., Roberts, D.A., 2014. Urban tree species mapping using hyperspectral and lidar data fusion. Remote Sens. Environ. 148, 70–83. https://doi.org/10.1016/j.rse.2014.03.018.

Asner, G., Martin, R., 2008. Spectral and chemical analysis of tropical forests: scaling from leaf to canopy levels. Remote Sens. Environ. 112, 3958–3970. https://doi.org/10.1016/j.rse.2008.07.003.

Asner, G.P., Martin, R.E., Anderson, C.B., Knapp, D.E., 2015. Quantifying forest canopy traits: imaging spectroscopy versus field survey. Remote Sens. Environ. 158, 15–27. https://doi.org/10.1016/j.rse.2014.11.011.

Blackburn, G.A., 1998. Spectral indices for estimating photosynthetic pigment concentrations: a test using senescent tree leaves. Int. J. Remote Sens. 19, 657–675. https://doi.org/10.1080/014311698215919.

Bond, B.J., 2000. Age-related changes in photosynthesis of woody plants. Trends Plant Sci. 5, 349–353. https://doi.org/10.1016/S1360-1385(00)01691-5.

Cavender-Bares, J., Schneider, F.D., Santos, M.J., et al., 2022. Integrating remote sensing with ecology and evolution to advance biodiversity conservation. Nat. Ecol. Evol. 6, 506–519. https://doi.org/10.1038/s41559-022-01702-5.

Chen, J.M., 1996. Evaluation of vegetation indices and a modified simple ratio for boreal applications. Can. J. Remote. Sens. 22, 229–242. https://doi.org/10.1080/07038992.1996.10855178.

Chen, L., Zhang, Y., Nunes, M.H., Stoddart, J., Khoury, S., Chan, A.H.Y., Coomes, D.A., 2022. Predicting leaf traits of temperate broadleaf deciduous trees from hyperspectral reflectance: can a general model be applied across a growing season? Remote Sens. Environ. 269, 112767. https://doi.org/10.1016/j.rse.2021.112767.

Chiarenza, G.M., Slavich, E., Moles, A.T., 2024. Guidelines for quantifying leaf chlorophyll content via non-destructive spectrometry. Appl. Plant Sci. 12, e11610. https://doi.org/10.1002/aps3.11610.

Chou, S., Chen, B., Chen, J., Wang, M., Wang, S., Croft, H., Shi, Q., 2020. Estimation of leaf photosynthetic capacity from the photochemical reflectance index and leaf pigments. Ecol. Indic. 110, 105867. https://doi.org/10.1016/j.ecolind.2019.105867.

Coopman, R.E., Briceño, V.F., Corcuera, L.J., Reyes-Díaz, M., Alvarez, D., Sáez, K., García-Plazaola, J.I., Alberdi, M., Bravo, L.A., 2011. Tree size and light availability increase photochemical instead of non-photochemical capacities of *Nothofagus nitida* trees growing in an evergreen temperate rain forest. Tree Physiol. 31, 1128–1141. https://doi.org/10.1093/treephys/tpr094.

Croft, H., Chen, J.M., 2018. Leaf Pigment Content. Comprehensive Remote Sensing. 117–142. https://doi.org/10.1016/b978-0-12-409548-9.10547-0.

Croft, H., Chen, J.M., Zhang, Y., 2014. The applicability of empirical vegetation indices for determining leaf chlorophyll content over different leaf and canopy structures. Ecol. Complex. 17, 119–130. https://doi.org/10.1016/j.ecocom.2013.11.005.

Croft, H., Chen, J.M., Luo, X., Bartlett, P., Chen, B., Staebler, R.M., 2017. Leaf chlorophyll content as a proxy for leaf photosynthetic capacity. Glob. Chang. Biol. 23, 3513–3524. https://doi.org/10.1111/gcb.13599.

Croft, H., Chen, J.M., Wang, R., Mo, G., Luo, S., Luo, X., He, L., Gonsamo, A., Arabian, J., Zhang, Y., Simic-Milas, A., Noland, T.L., He, Y., Homolová, L., Malenovský, Z., Yi, Q., Beringer, J., Amiri, R., Hutley, L., Arellano, P., Stahl, C., Bonal, D., 2020. The global distribution of leaf chlorophyll content. Remote Sens. Environ. 236, 111479. https://doi.org/10.1016/j.rse.2019.111479.

Dalponte, M., 2018. itcSegment: Individual Tree Crowns Segmentation. R Package Version 0.8. 2018. Available online. https://CRAN.R-project.org/package=itcSegment. accessed on 22 April 2026.

Dalponte, M., Reyes, F., Kandare, K., Gianelle, D., 2015. Delineation of individual tree crowns from ALS and hyperspectral data: a comparison among four methods. Eur. J. Remote Sens. 48, 365–382. https://doi.org/10.5721/EuJRS20154821.

Dasgupta, P., 2021. The Economics of Biodiversity: The Dasgupta Review. HM Treasury, London.
Datt, B., 1999. Visible/near infrared reflectance and chlorophyll content in *Eucalyptus* leaves. Int. J. Remote Sens. 20, 2741–2759. https://doi.org/10.1080/014311699211778.
Deepak, M., Keski-Saari, S., Fauch, L., Granlund, L., Oksanen, E., Keinänen, M., 2020. Spectral reflectance in silver birch genotypes from three provenances in Finland. Remote Sens. 12, 2677. https://doi.org/10.3390/rs12172677.
Esteban, R., Barrutia, O., Artetxe, U., Fernández-Marín, B., Hernández, A., García-Plazaola, J.I., 2015. Internal and external factors affecting photosynthetic pigment composition in plants: a meta-analytical approach. New Phytol. 206, 268–280. https://doi.org/10.1111/nph.13186.
Evans, J.R., Poorter, H., 2001. Photosynthetic acclimation of plants to growth irradiance: the relative importance of specific leaf area and nitrogen partitioning in maximizing carbon gain. Plant Cell Environ. 24, 755–767. https://doi.org/10.1046/j.1365-3040.2001.00724.x.
Gates, D.M., Keegan, H.J., Schleter, J.C., Weidner, V.R., 1965. Spectral properties of plants. Appl. Opt. 4, 11–20. https://doi.org/10.1364/AO.4.000011.
Geladi, P., MacDougall, D., Martens, H., 1985. Linearization and scatter-correction for near-infrared reflectance spectra of meat. Appl. Spectrosc. 39, 491–500.
Hardenbol, A.A., Junninen, K., Kouki, J., 2020. A key tree species for forest biodiversity, European aspen (*Populus tremula*), is rapidly declining in boreal old-growth forest reserves. For. Ecol. Manag. 462, 118009. https://doi.org/10.1016/j.foreco.2020.118009.
Hashimoto, H., Uragami, C., Cogdell, R.J., 2016. Carotenoids and photosynthesis. In: Stange, C. (Ed.), Carotenoids in Nature: Biosynthesis, Regulation and Function, Subcellular Biochemistry. Springer International Publishing, Cham, pp. 111–139. https://doi.org/10.1007/978-3-319-39126-7_4.
He, C., Sun, J., Chen, Y., Wang, L., Shi, S., Qiu, F., Wang, S., Tagesson, T., 2023. A new vegetation index combination for leaf carotenoid-to-chlorophyll ratio: minimizing the effect of their correlation. Int. J. Digit. Earth 16, 272–288. https://doi.org/10.1080/17538947.2023.2168772.
Hoeppner, J.M., Skidmore, A.K., Darvishzadeh, R., Heurich, M., Chang, H.-C., Gara, T. W., 2020. Mapping canopy chlorophyll content in a temperate forest using airborne hyperspectral data. Remote Sens. 12, 3573. https://doi.org/10.3390/rs12213573.
Kamoske, A.G., Dahlin, K.M., Serbin, S.P., Stark, S.C., 2021. Leaf traits and canopy structure together explain canopy functional diversity: an airborne remote sensing approach. Ecol. Appl. 31, e02230. https://doi.org/10.1002/eap.2230.
Kivinen, S., Koivisto, E., Keski-Saari, S., Poikolainen, L., Tanhuanpää, T., Kuzmin, A., Viinikka, A., Heikkinen, R.K., Pykälä, J., Virkkala, R., Vihervaara, P., Kumpula, T., 2020. A keystone species, European aspen (*Populus tremula* L.), in boreal forests: ecological role, knowledge needs and mapping using remote sensing. For. Ecol. Manag. 462, 118008. https://doi.org/10.1016/j.foreco.2020.118008.
Koricheva, J., Hayes, D., 2018. The relative importance of plant intraspecific diversity in structuring arthropod communities: a meta-analysis. Funct. Ecol. 32, 1704–1717. https://doi.org/10.1111/1365-2435.13062.
Kouki, J., Arnold, K., Martikainen, P., 2004. Long-term persistence of aspen – a key host for many threatened species – is endangered in old-growth conservation areas in Finland. J. Nat. Conserv. 12, 41–52. https://doi.org/10.1016/j.jnc.2003.08.002.
Kull, O., Tulva, I., 2000. Modelling canopy growth and steady-state leaf area index in an aspen stand. Ann. For. Sci. 57, 611–621. https://doi.org/10.1051/forest:2000130.
Kusbach, A., Šebesta, J., Hruban, R., Peška, P., Rogers, P.C., 2024. Eurasian aspen (*Populus tremula* L.): central Europe's keystone species 'hiding in plain sight.'. PLoS One 19, e0301109. https://doi.org/10.1371/journal.pone.0301109.
Lankia, H., Wallenius, T., Várkonyi, G., Kouki, J., Snäll, T., 2012. Forest fire history, aspen and goat willow in a Fennoscandian old-growth landscape: are current population structures a legacy of historical fires? J. Veg. Sci. 23, 1159–1169. https://doi.org/10.1111/j.1654-1103.2012.01426.x.
LaRue, E.A., Knott, J.A., Domke, G.M., Chen, H.Y., Guo, Q., Hisano, M., Oswalt, C., Oswalt, S., Kong, N., Potter, K.M., Fei, S., 2023. Structural diversity as a reliable and novel predictor for ecosystem productivity. Front. Ecol. Environ. 21, 33–39. https://doi.org/10.1002/fee.2586.
Latva-Karjanmaa, T., Penttilä, R., Siitonen, J., 2007. The demographic structure of European aspen (*Populus tremula*) populations in managed and old-growth boreal forests in eastern Finland. Can. J. For. Sci. 37, 1070–1081.
Li, Y., Liu, C., Zhang, J., Yang, H., Xu, L., Wang, Q., Sack, L., Wu, X., Hou, J., He, N., 2018a. Variation in leaf chlorophyll concentration from tropical to cold-temperate forests: association with gross primary productivity. Ecol. Indic. 85, 383–389. https://doi.org/10.1016/j.ecolind.2017.10.025.
Li, Y., He, N., Hou, J., Xu, L., Liu, C., Zhang, J., Wang, Q., Zhang, X., Wu, X., 2018b. Factors influencing leaf chlorophyll content in natural forests at the biome scale. Front. Ecol. Evol. 6. https://doi.org/10.3389/fevo.2018.00064.
Li, J., Yu, P., Wan, Y., Wang, Y., Liu, B., Yu, Y., 2023. Effects of topography and social position on the solar radiation of individual trees on a hillslope in northwest China. Forests 14, 561. https://doi.org/10.3390/f14030561.
Lichtenthaler, H.K., Buschmann, C., 2001. Chlorophylls and carotenoids: measurement and characterization by UV-VIS spectroscopy. Curr. Protocols Food Anal. Chem. 1. https://doi.org/10.1002/0471142913.faf0403s01. F4.3.1-F4.3.8.
Lichtenthaler, H.K., Ač, A., Marek, M.V., Kalina, J., Urban, O., 2007. Differences in pigment composition, photosynthetic rates and chlorophyll fluorescence images of sun and shade leaves of four tree species. Plant Physiol. Biochem. 45, 577–588. https://doi.org/10.1016/j.plaphy.2007.04.006.
Lieffers, V.J., Pinno, B.D., Stadt, K.J., 2002. Light dynamics and free-to-grow standards in aspen-dominated mixedwood forests. For. Chron. 78, 137–145. https://doi.org/10.5558/tfc78137-1.
Lin, Q., Huang, H., Wang, J., Huang, K., Liu, Y., 2019. Detection of pine shoot beetle (PSB) stress on pine forests at individual tree level using UAV-based hyperspectral imagery and Lidar. Remote Sens. 11, 2540. https://doi.org/10.3390/rs11212540.
Linder, P., Elfving, B., Zackrisson, O., 1997. Stand structure and successional trends in virgin boreal forest reserves in Sweden. For. Ecol. Manag. 98, 17–33. https://doi.org/10.1016/S0378-1127(97)00076-5.
Lundberg, S.M., Lee, S.-I., 2017. A unified approach to interpreting model predictions. In: Advances in Neural Information Processing Systems. Curran Associates, Inc.
Lundberg, S.M., Erion, G.G., Lee, S.-I., 2019. Consistent individualized feature attribution for tree ensembles. arXiv, 1802.03888v3 [cs.LG] Latest viewed on 27.05.2026.
Madritch, M.D., Kingdon, C.C., Singh, A., Mock, K.E., Lindroth, R.L., Townsend, P.A., 2014. Imaging spectroscopy links aspen genotype with below-ground processes at landscape scales. Philos. Transact. R. Soc. B Biol. Sci. 369.
Mäyrä, J., Keski-Saari, S., Kivinen, S., Tanhuanpää, T., Hurskainen, P., Kullberg, P., Poikolainen, L., Viinikka, A., Tuominen, S., Kumpula, T., Vihervaara, P., 2021. Tree species classification from airborne hyperspectral and LiDAR data using 3D convolutional neural networks. Remote Sens. Environ. 256, 112322. https://doi.org/10.1016/j.rse.2021.112322.
Minocha, R., Martinez, G., Lyons, B., Long, S., 2009. Development of a standardized methodology for quantifying total chlorophyll and carotenoids from foliage of hardwood and conifer tree species. Can. J. For. Res. 39, 849–861. https://doi.org/10.1139/X09-015.
Nestola, E., Scartazza, A., Di Baccio, D., Castagna, A., Ranieri, A., Cammarano, M., Mazzenga, F., Matteucci, G., Calfapietra, C., 2018. Are optical indices good proxies of seasonal changes in carbon fluxes and stress-related physiological status in a beech forest? Sci. Total Environ. 612, 1030–1041. https://doi.org/10.1016/j.scitotenv.2017.08.167.
Niinemets, Ü., 2010. A review of light interception in plant stands from leaf to canopy in different plant functional types and in species with varying shade tolerance. Ecol. Res. 25, 693–714. https://doi.org/10.1007/s11284-010-0712-4.
Paillet, Y., Archaux, F., Boulanger, V., Debaive, N., Fuhr, M., Gilg, O., Gosselin, F., Guilbert, E., 2017. Snags and large trees drive higher tree microhabitat densities in strict forest reserves. For. Ecol. Manag. 389, 176–186. https://doi.org/10.1016/j.foreco.2016.12.014.
Palmroos, I., Norros, V., Keski-Saari, S., Mäyrä, J., Tanhuanpää, T., Kivinen, S., Pykälä, J., Kullberg, P., Kumpula, T., Vihervaara, P., 2023. Remote sensing in mapping biodiversity – A case study of epiphytic lichen communities. For. Ecol. Manag. 538, 120993. https://doi.org/10.1016/j.foreco.2023.120993.
Pedregosa, F., Varoquaux, G., Gramfort, A., Michel, V., Thirion, B., Grisel, O., Blondel, M., Prettenhofer, P., Weiss, R., Dubourg, V., Vanderplas, J., Passos, A., Cournapeau, D., Brucher, M., Perrot, M., Duchesnay, É., 2011. Scikit-learn: machine learning in Python. J. Mach. Learn. Res. 12, 2825–2830.
Richter, R., Schläpfer, D., 2002. Geo-atmospheric processing of airborne imaging spectrometry data. Part 2: atmospheric/topographic correction. Int. J. Remote Sens. 23, 2631–2649. https://doi.org/10.1080/01431160110115834.
Rogers, P.C., Pinno, B.D., Šebesta, J., Albrectsen, B.R., Li, G., Ivanova, N., Kusbach, A., Kuuluvainen, T., Landhäusser, S.M., Liu, H., Myking, T., Pulkkinen, P., Wen, Z., Kulakowski, D., 2020. A global view of aspen: conservation science for widespread keystone systems. Global Ecol. Conserv. 21, e00828. https://doi.org/10.1016/j.gecco.2019.e00828.
Rozendaal, D.M.A., Hurtado, V.H., Poorter, L., 2006. Plasticity in leaf traits of 38 tropical tree species in response to light; relationships with light demand and adult stature. Funct. Ecol. 20, 207–216. https://doi.org/10.1111/j.1365-2435.2006.01105.x.
Schläpfer, D., Richter, R., 2002. Geo-atmospheric processing of airborne imaging spectrometry data. Part 1: parametric orthorectification. Int. J. Remote Sens. 23, 2609–2630. https://doi.org/10.1080/01431160110115825.
Serbin, S.P., Singh, A., McNeil, B.E., Kingdon, C.C., Townsend, P.A., 2014. Spectroscopic determination of leaf morphological and biochemical traits for northern temperate and boreal tree species. Ecol. Appl. 24, 1651–1669. https://doi.org/10.1890/13-2110.1.
Sims, D.A., Gamon, J.A., 2002. Relationships between leaf pigment content and spectral reflectance across a wide range of species, leaf structures and developmental stages. Remote Sens. Environ. 81, 337–354. https://doi.org/10.1016/S0034-4257(02)00010-X.
Skidmore, A.K., Coops, N.C., Neinavaz, E., Ali, A., Schaepman, M.E., Paganini, M., Kissling, W.D., Vihervaara, P., Darvishzadeh, R., Feilhauer, H., Fernandez, M., Fernández, N., Gorelick, N., Geijzendorffer, I., Heiden, U., Heurich, M., Hobern, D., Holzwarth, S., Muller-Karger, F.E., Van De Kerchove, R., Lausch, A., Leitão, P.J., Lock, M.C., Mücher, C.A., O'Connor, B., Rocchini, D., Roeoesli, C., Turner, W., Vis, J. K., Wang, T., Wegmann, M., Wingate, V., 2021. Priority list of biodiversity metrics to observe from space. Nat. Ecol. Evol. 5, 896–906. https://doi.org/10.1038/s41559-021-01451-x.
Spasojevic, M.J., Turner, B.L., Myers, J.A., 2016. When does intraspecific trait variation contribute to functional beta-diversity? J. Ecol. 104, 487–496.
Suvanto, L.I., Latva-Karjanmaa, T.B., 2005. Clone identification and clonal structure of the European aspen (*Populus tremula*). Mol. Ecol. 14, 2851–2860. https://doi.org/10.1111/j.1365-294X.2005.02634.x.
Tikkanen, O.-P., Martikainen, P., Hyvärinen, E., Junninen, K., Kouki, J., 2006. Red-listed boreal forest species of Finland: associations with forest structure, tree species, and decaying wood. Ann. Bot. Fenn. 43, 373–383.
Tsuchiya, Y., Hirono, Y., Sonobe, R., 2025. Estimating chlorophyll content in tea leaves using spectral reflectance and deep learning methods. Ecol. Inform. 91, 103399. https://doi.org/10.1016/j.ecoinf.2025.103399.
Viinikka, A., Hurskainen, P., Keski-Saari, S., Kivinen, S., Tanhuanpää, T., Mäyrä, J., Poikolainen, L., Vihervaara, P., Kumpula, T., 2020. Detecting European aspen

(*Populus tremula* L.) in boreal forests using airborne hyperspectral and airborne laser scanning data. Remote Sens. 12, 2610. https://doi.org/10.3390/rs12162610.

Virtanen, P., Gommers, R., Oliphant, T.E., Haberland, M., Reddy, T., Cournapeau, D., Burovski, E., Peterson, P., Weckesser, W., Bright, J., van der Walt, S.J., Brett, M., Wilson, J., Millman, K.J., Mayorov, N., Nelson, A.R.J., Jones, E., Kern, R., Larson, E., Carey, C.J., Polat, İ., Feng, Y., Moore, E.W., VanderPlas, J., Laxalde, D., Perktold, J., Cimrman, R., Henriksen, I., Quintero, E.A., Harris, C.R., Archibald, A.M., Ribeiro, A. H., Pedregosa, F., van Mulbregt, P., 2020. SciPy 1.0: fundamental algorithms for scientific computing in Python. Nat. Methods 17, 261–272. https://doi.org/10.1038/s41592-019-0686-2.

Whitham, T.G., Bailey, J.K., Schweitzer, J.A., Shuster, S.M., Bangert, R.K., LeRoy, C.J., Lonsdorf, E.V., Allan, G.J., DiFazio, S.P., Potts, B.M., Fischer, D.G., Gehring, C.A., Lindroth, R.L., Marks, J.C., Hart, S.C., Wimp, G.M., Wooley, S.C., 2006. A framework for community and ecosystem genetics: from genes to ecosystems. Nat. Rev. Genet. 7, 510–523. https://doi.org/10.1038/nrg1877.

Zarco-Tejada, P.J., Miller, J.R., Mohammed, G.H., Noland, T.L., Sampson, P.H., 2002. Vegetation stress detection through chlorophyll a + b estimation and fluorescence effects on hyperspectral imagery. J. Env. Quality 31, 1433–1441.

Zarco-Tejada, P.J., Berjón, A., López-Lozano, R., Miller, J.R., Martín, P., Cachorro, V., González, M.R., de Frutos, A., 2005. Assessing vineyard condition with hyperspectral indices: leaf and canopy reflectance simulation in a row-structured discontinuous canopy. Remote Sens. Environ. 99, 271–287. https://doi.org/10.1016/j.rse.2005.09.002.

Zhao, Y., Zeng, Y., Zheng, Z., Dong, W., Zhao, D., Wu, B., Zhao, Q., 2018. Forest species diversity mapping using airborne LiDAR and hyperspectral data in a subtropical forest in China. Remote Sens. Environ. 213, 104–114. https://doi.org/10.1016/j.rse.2018.05.014.